Combining doubly charged cations and anions to form new species

Nick Gonzales and Jack Simons
Chemistry Department, University of Utah, Salt Lake City, Utah 84112

(Received 25 October 1993; accepted 29 December 1993)

In this study we predict, based on our *ab initio* electronic structure calculations, the existence and relative stabilities of several new species such as H_3SMgF_3, H_2SMgF_2, and HSMgF derived from combining the geometrically metastable and electronically stable parent doubly charged ions H_4S^{+2} and MgF_4^{-2}. Although this study focuses on compounds obtained from these particular double ions, we suggest that analogous observations will be obtained when other double ions are used. Stable structures of the HSMgF, and H_2SMgF_2 molecules, as well as a local energy minimum and two different second-order saddle point geometries for the H_3SMgF_3 molecule were found. The lowest-energy stable structure is that found for H_3SMgF_3, which is best described as a dative adduct of H_2S, MgF_2, and HF, and which lies ~570 kcal/mol below the separated-ion starting materials and ~140 kcal/mol below the $(H_4S^{+2})(MgF_4^{-2})$ contact ion pair.

I. INTRODUCTION

Our earlier work[1] on multiprotonated doubly charged cations MH_n^{+2} and work of our group and others[2] on doubly charged anions involving MF_m^{-2} stoichiometry has lead us to examine compounds that use these types of ions as "building blocks." In particular, we consider in this paper "salts" such as H_4S^{+2} MgF_4^{-2} that might be formed by combining a pair[3] of double ions of opposite charge for which energy considerations retain their +2/−2 charge separation.

Although our attention in this paper is limited to $H_4S^{+2}+MgF_4^{-2}$ prototype systems, one can imagine (and we intend to examine) numerous other such ion pairs. We made these choices both because earlier work[1,2(e)] on H_4S^{+2} and MgF_4^{-2} was available to guide us and because the covalent and ionic radii of the atoms involved suggesting that steric or "packing" effects would not hinder the bonding arrangements we wanted to study for these particular atoms.

In several of the species examined in this study, the extended valence of the Mg and S atoms, as well as the large electronegativity difference between the Mg and S atoms and the ligands bound to them, gives rise to a high degree of internal charge separation. For example, in H_3SMgF_3, the H atoms each possess charges near +2/3 and the F atoms each have charges near −2/3. As noted earlier,[1] it is the resonance delocalization of the +2 and −2 charges over more than two ligands that provides much of these species' geometrical and electronic stability to electron detachment.

A. Double ions contain much energy

One aspect of the large internal charge separation contained in our systems makes their study especially interesting to us. This is the very large "pent up" Coulombic energy that earlier findings[1,2] lead us to believe may be released if the materials are heated (so that activation barriers to intramolecular decomposition are overcome) or photolyzed (so dissociative excited electronic states are accessed).

To illustrate the energy content of one such ion, we review what was found in Ref. 1 with respect to the H_4S^{+2} ion depicted in Fig. 1. The energy of the $^1A_1$ ground-state electronic energy of this ion is shown in Fig. 2 as a function of one of the S–H bond lengths R(SH), with the other three bond lengths and all internal angles optimized to produce the lowest possible energy for each R(SH). Analogous findings pertain to dianions such as F_4Mg^{-2} shown in Fig. 3.

The essential features contained in Fig. 2, and which generalize[1,2] to findings on other dications and dianions, are:

1. *Local minima* on the potential energy surfaces do indeed exist even for isolated doubly charged ions.
2. These local minima have energies very much in excess of the global minima corresponding to two separated singly charged ions (e.g., $H^+ + H_3S^+$ in the H_4S^{+2} case).
3. Substantial barriers exist to fragmentation of doubly charged ions. These barriers are especially "wide" because of the Coulomb nature of the potential at long range, which causes the tunneling lifetimes to be especially long.
4. Delocalization of the double charge over more than two atomic centers contributes to the stabilization of these species.

B. Energy barriers make these double ions geometrically metastable

The energy content of doubly charged ions as well as the barriers that must be overcome to effect fragmentation can be quite large. To illustrate, we show, in Table I, the computed dissociation energies (negative numbers implying exothermic reaction) and barriers to dissociation for a group of doubly charged ions studied earlier.[1,2] The exothermicities range from 29 to 115 kcal/mol and the barriers, where known, range from 5 to 56 kcal/mol.

C. These dianions do not have low electron detachment energies

The electronic stability of several dianions with respect to loss of a single electron (e.g., $F_4Mg^{-2} \rightarrow F_4Mg^- + e^-$) has been examined in earlier work[2(e)] and found to be substantial (see Table II). For example, for F_4Mg^{-2} the vertical electron detachment energy (DE) is 2.98 eV, and for TeF_8^{-2} it is pre-

 0021-9606/94/100(8)/5778/7/$6.00

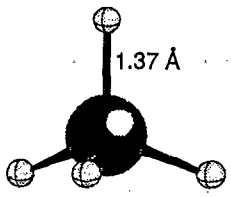

FIG. 1. Tetrahedral equilibrium geometry of the H_4S^{+2} dication.

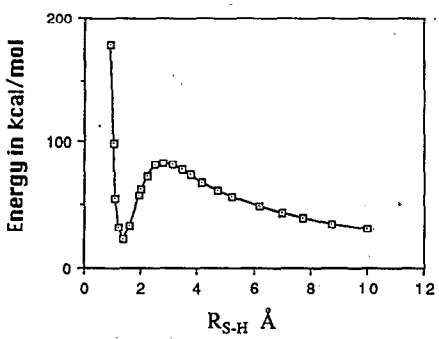

FIG. 2. The SCF/6-31++G** ground-state electronic energy (including nuclear repulsion) of H_4S^{2+} as a function of *one* S–H bond length with the remaining internal coordinates optimized to produce a minimum energy path.

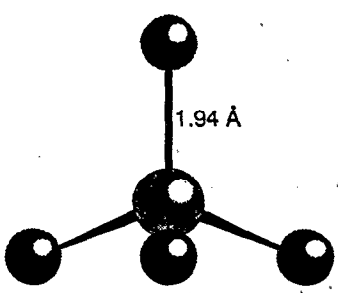

FIG. 3. Tetrahedral equilibrium geometry of the F_4Mg^{-2} dianion.

TABLE I. Calculated dissociation energies (ΔE) and dissociation barriers ($E^{\dagger}$) (kcal/mol) for doubly charged ions.

Species	ΔE	$E^{\dagger}$
$H_4O^{2+} \rightarrow H_3O^+ + H^+$	-61^a	38
$H_3F^{2+} \rightarrow H_2F^+ + H^+$	-111^a	12
$H_4S^{2+} \rightarrow H_3S^+ + H^+$	-29^a	56
$H_3Cl^{2+} \rightarrow H_2Cl^+ + H^+$	-67^a	34
$H_2Ar^{2+} \rightarrow HAr^+ + H^+$	-115^a	5
$F_4Be^{2-} \rightarrow F_3Be^- + F^-$	-82^b	14
$F_4Mg^{2-} \rightarrow F_3Mg^- + F^-$	-31^c	24
$F_8Te^{2-} \rightarrow F_7Te^- + F^-$	-43^d	?
$Cl_8Te^{2-} \rightarrow Cl_7Te^- + Cl^-$	-69^d	?
$F_8Se^{2-} \rightarrow F_7Se^- + F^-$	-75^d	?

[a]Reference 1.
[b]Reference 2(a).
[c]Reference 2(e).
[d]Reference 2(b).

TABLE II. Vertical electron detachment energies (DE) (eV) at Koopmans' theorem and correlated levels of theory.

Species	Koopmans' DE	Correlated DE
F_4Be^{2-}	3.5^a	1.9
F_4Mg^{2-}	4.4^b	3.0
F_6Se^{2-}	5.4^c	3.8
F_8Te^{2-}	6.5^c	5.0
F_8Se^{2-}	5.5^c	?
Cl_8Te^{2-}	3.9^c	?
F_7Te^{2-}	11.9^c	?
F_7Se^{2-}	11.2^c	?
Cl_7Te^{2-}	8.0^c	?

[a]Reference 2(a).
[b]Reference 2(e).
[c]Reference 2(b).

dicted to be approximately 5 eV. These results imply that such dianions may exist in close proximity to cations or other species with rather substantial oxidizing strength.

D. Dications have large oxidation power

The electron attachment energies of several dications have been determined and several are summarized in Table III. It should be noted that the adiabatic electron attachment energies (ΔE_{ad}), which correspond to addition of an electron followed by loss of one H atom (since this is energetically favored and occurs spontaneously):

$$H_nM^{2+} + e^- \rightarrow H + H_{(n-1)}M^+$$

are considerably larger than the vertical energies (ΔE_v) corresponding to the simple addition of an electron at the (frozen) geometry of the dication:

$$H_nM^{2+} + e^- \rightarrow H_nM^+.$$

However, the vertical energies provide a measure of the dications' ability to "pull" an electron away from a neighboring species; subsequent to acquiring an electron the nascent mono-cation will decompose releasing an amount of energy equal to $\Delta E_{ad} - \Delta E_v$.

TABLE III. Vertical[a] (ΔE_v) and adiabatic[b] (ΔE_{ad}) electron attachment energies (eV) for dications.

	Reaction	ΔE^c(eV)
ΔE_v	$H_4O^{2+} + e \rightarrow H_4O^+$	13.2
ΔE_{ad}	$H_4O^{2+} + e \rightarrow H_3O^+ + H$	16.0
ΔE_v	$H_4S^{2+} + e \rightarrow H_4S^+$	14.0
ΔE_{ad}	$H_4S^{2+} + e \rightarrow H_3S^+ + H$	14.6
ΔE_v	$H_3F^{2+} + e \rightarrow H_3F^+$	15.4
ΔE_{ad}	$H_3F^{2+} + e \rightarrow H_2F^+ + H$	18.3
ΔE_v	$H_3Cl^{2+} + e \rightarrow H_3Cl^+$	13.3
ΔE_{ad}	$H_3Cl^{2+} + e \rightarrow H_2Cl^+ + H$	16.3
ΔE_v	$H_2Ar^{2+} + e \rightarrow H_2Ar^+$	15.1
ΔE_{ad}	$H_2Ar^{2+} + e \rightarrow HAr^+ + H$	18.5

[a]The vertical ΔE_v gives ΔE (ZPE-corrected) for the process $H_nM^{k+} + e \rightarrow H_nM^{(k-1)+}$ at the geometry of H_nM^{k+}.
[b]The adiabatic ΔE_{ad} gives ΔE (ZPE-corrected) for the process $H_nM^{k+} + e \rightarrow H + H_{(n-1)}M^{(k-1)+}$, in which $H_{(n-1)}M^{(k-1)+}$ is produced at its equilibrium geometry.
[c]Reference 1.

TABLE IV. Total and relative energies,[a] geometries, and vibrational frequencies for species relating to H_4S^{+2} using a 6-311++G** basis set.

Species	Point group	Energy (a.u.)	Relative energy (kcal/mol)	Distances (Å) and angles (deg)	Vib. freq. (cm^{-1}) ZPE(kcal/mol)	$E_{(LUMO)}$ (a.u.)	Atomic charges
H_4S^{+2}	T_d	−399.120 943	0	r=1.3784	T_2 1001 E 1209 T_2 2479 A_1 2484 /21.9	−0.3804	S=0.70 H=0.33 H=0.33 H=0.33 H=0.33
$\{H_3S\cdots H_a\}^{+2}$ Transition state	C_{3v}	−399.023 887	56	r_{SH_a}=2.8376 r_{SH}=1.3575 HSH_a=118.2 HSH=100.0	A_1 743i E 389 A_1 1029 E 1199 A_1 2638 E 2647 /17.4	−0.6104	S=0.32 H_a=0.91 H=0.26 H=0.26 H=0.26
H_3S^+ + H^+	C_{3v}	−399.158 895	−29	r=1.3465 HSH=95.9	A_1 1075 E 1233 A_1 2736 E 2746 /16.8	−0.1395	S=0.44 H=0.19 H=0.19 H=0.19

[a]All electronic energies in this and other tables, unless specified otherwise, are of MP4SDTQ quality.

The fact that there seem to be no barriers to dissociation of the H_nM^+ species means that we must be wary of processes that reduce the H_nM^{2+} species because the nascent H_nM^+ will no longer be geometrically stable. For example, in the $(F_4Mg^{-2})(H_4S^{+2})$ salt discussed later in this paper, we need to know the energy of the charge transfer $(F_4Mg^-)(H_4S^+)$ state, because such a transition would lead to fragmentation of the H_4S^+ moiety and of the F_4Mg^- ion.[2(e)]

This charge transfer energy could be estimated in terms of the vertical electron detachment energy (DE) of F_4Mg^{-2} (3.0 eV), the ΔE_v of H_4S^{+2} (14 eV), and the change in Coulombic attraction accompanying the

$$(F_4Mg^{-2})(H_4S^{+2})\rightarrow(F_4Mg^-)(H_4S^+)$$

process. The latter energy is approximately $(4-1)e^2/R$, where R is the interionic distance in the salt.[4] Unfortunately, this means of estimating the transition energy depends upon

TABLE V. Total and relative energies, geometries, and vibrational frequencies for species relating to MgF_4^{-2} using a 6-311++G** basis set.

Species	Point group	Energy (a.u.)	Relative energy (kcal)	Distances (Å) and angles (deg)	Vib. freq. (cm^{-1}) /ZPE (kcal)	$E_{(HOMO)}$ (a.u.)	Atomic charges
MgF_4^{-2}	T_d	−598.612 088	0	r=1.9483	E 137 T_2 223 A_1 382 T_2 492 /4.0	−0.1644	Mg=1.11 F=−0.78 F=−0.78 F=−0.78 F=−0.78
$\{F_3Mg\cdots F_a\}^{-2}$ Transition state	C_{3v}	−598.573 046	24	r_{MgF_a}=3.817 r_{MgF}=1.8789 $FMgF_a$=101.5 FMgF=116.0	A_1 89i E 83 E 192 A_1 240 A_1 454 E 604 /3.5	−0.1019	Mg=1.11 F_a=−0.98 F=−0.72 F=−0.72 F=−0.72
F_3Mg^- + F^-	D_{3h}	−498.976 324 + −99.684 425	−31	r=1.8252	E' 182 A_2'' 249 A_1' 468 E' 655 /3.4	−0.3518	Mg=1.01 F=−0.67 F=−0.67 F=−0.67

TABLE VI. Total energies and vibrational frequencies for species relating to the $H_4S^{+2}+MgF_4^{-2}$ reaction using a 6-311++G** basis set.

Species	Point group	MP4 energy (a.u.)	Vib. freq. (cm^{-1}) /ZPE (kcal/mol)			$E_{(HOMO)}-E_{(LUMO)}$ (kcal/mol)	Atomic charges
$MgF_4^{-2}+H_4S^{+2}$		−997.715 031				135	Tables IV and V
$(MgF_4^{-2})(H_4S^{+2})$	C_{3v}	−998.422 181[a]				264	
H_3SMgF_3	C_{3v}	−898.280 3336	E 178i		A_1 519	313	S=0.38
(H not inverted)			A_2 140		E 635		Mg=0.96
(F inverted)			E 172		A_1 1090		H=0.16
(staggered)			A_1 177		E 1237		F=−0.61
			E 229		A_1 2751		
			A_1 256		E 2775		
				/20.4			
H_3SMgF_3	C_{3v}	−898.321 7267	E 174i		A_1 527	322	S=0.15
(both inverted)			E 192		E 632		Mg=0.94
			A_1 228		A_1 1154		H=0.19
			A_1 297		E 1195		F=−0.55
			E 498		E 2110		
			A_1 502		A_1 2272		
				/20.4			
H_3SMgF_3	C_1	−898.353 1117	47	239	854	287	S=−0.08
(true minimum)			106	325	979		Mg=1.04
			128	366	1209		H=0.16
			187	442	2670		H=0.09
			202	537	2815		H=0.14
+		+	211	788	2955		F=−0.20
				/21.5			F=−0.58
							F=−0.57
HF		−100.286 2321		4200			
				/6.0			
H_2SMgF_2	C_s	−798.044 7997	A'' 30		A'' 443	301	S=0.07
			A'' 100		A' 534		Mg=0.92
+		+	A' 144		A'' 814		H=0.07
			A' 151		A' 1192		H=0.07
			A' 255		A' 2803		F=−0.57
2HF		−200.572 4642	A' 365		A'' 2819		F=−0.57
				/13.8			
HSMgF	C_s	697.719 2727	A' 120		A' 562	237	S=−0.26
			A'' 126		A' 763		Mg=0.78
+		+	A' 380		A' 2775		H=0.00
				/6.8			F=−0.53
3HF		−300.858 6963					

[a]This calculation was done at the MP4SDQ level because the MP4SDTQ calculation was not feasible.

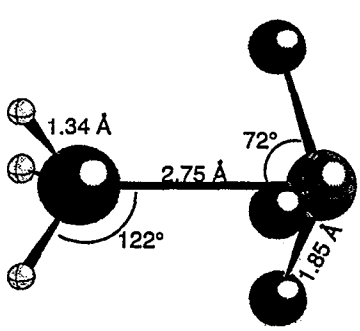

FIG. 4. A second-order saddle point of H_3SMgF_3 where the fluorines are inverted, the hydrogens are not, and the ligands are staggered. This structure has C_{3v} symmetry and is 46 kcal/mol above the minimum shown in Fig. 6.

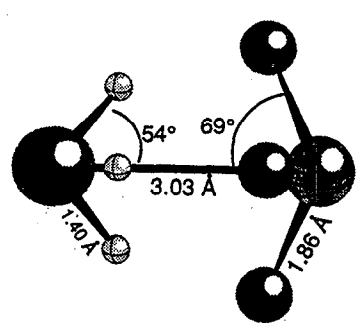

FIG. 5. Another second-order saddle point geometry (C_{3v}) of H_3SMgF_3 which is 20 kcal/mol above the minimum shown in Fig. 6.

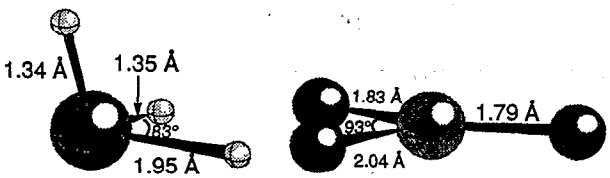

FIG. 6. Equilibrium structure of H_3SMgF_3. R_{S-Mg}=3.99 Å.

knowing the F^- ionic radius, which limits its accuracy. Hence, we simply calculated the HOMO-LUMO energy gap for the $(F_4Mg^{-2})(H_4S^{+2})$ dimer with tetrahedral internal ion geometries to simulate the presumed structures in the solid, and obtained 264 kcal/mol.

E. Metastability and high-energy content present challenges

Clearly, much energy is stored in these ions and, for some of the species, the barriers are large enough to render the ions stable over long times. The shortest lived are likely to be the multiprotonated species where the H nuclei can tunnel through or be energized over the barriers; the multifluorinated anions are likely to be much more geometrically stable. For the prototypical cation–anion pair that is the focal point of the present study, H_4S^{+2} and F_4Mg^{-2}, the Coulomb explosion exothermicities and barriers are

$$H_4S^{+2} \rightarrow H_3S^+ + H^+; \quad \Delta E = -29 \text{ kcal/mol};$$

$$E^\dagger = 56 \text{ kcal/mol}$$

and

$$F_4Mg^{-2} \rightarrow F_3Mg^- + F^-; \quad \Delta E = -31 \text{ kcal/mol};$$

$$E^\dagger = 24 \text{ kcal/mol}.$$

These barriers are large enough to render both species very stable.

II. COMPUTATIONAL DETAILS

Rather straightforward *ab initio* theoretical methods were employed to carry out most of the calculations whose results are reported here. All geometries were first optimized using analytical self-consistent field (SCF) gradients with polarized triply split-valence basis sets.[5] Further refined geometries were obtained using second-order Møller–Plesset perturbation theory.

The fundamental vibrational frequencies, normal coordinates, and zero-point energies (ZPE) were calculated by standard matrix methods. Finally, correlated total energies at the critical geometries (i.e., local minima and barriers) were evaluated using full fourth-order frozen-core approximation Møller–Plesset perturbation theory. The GAUSSIAN92 program suite[6] was used to perform all of the calculations whose results are discussed here.

III. FINDINGS

A. The H_4S^{+2} and MgF_4^{-2} ions

In Table IV we summarize the geometry and energetic data found for H_4S^{+2}, along with the corresponding local harmonic vibrational frequencies. Table V contains analogous data for MgF_4^{-2}. Also shown are the highest occupied (for MgF_4^{-2}) and lowest unoccupied (for H_4S^{+2}) molecular orbital energies and the Mulliken charge densities on each atomic center. The latter clearly display sharp changes when passing through the barrier regions, and show the high degree of internal charge separation and delocalization.

B. The $(H_4S^{+2})(MgF_4^{-2})$ salt and H_3SMgF_3 structures

In Table VI we provide structural and energetic data for the separated ions $MgF_4^{-2}+H_4S^{+2}$, the contact ion pair $(MgF_4^{-2})(H_4S^{+2})$, and several H_3SMgF_3 structures formed by HF elimination. The geometries of three H_3SMgF_3 species are shown in Figs. 4, 5, and 6.

The first H_3SMgF_3 structure we found is shown in Fig. 4, which was obtained when we constrained the geometry optimization algorithm to maintain a C_3 symmetry axis. This structure has the H–S bonds pointing away from the fluorine atoms. We began this optimization with both portions of the molecule directed outward (i.e., in the usual way expected by hybridization) but the energy minimizing process converged to a structure which turns out to be a second-order saddle point on the potential energy surface, and the imaginary frequencies (178 cm^{-1}) correspond to a degenerate distortion of the molecule. This isomer is 46 kcal/mol higher in energy than the minimum energy structure discussed below.

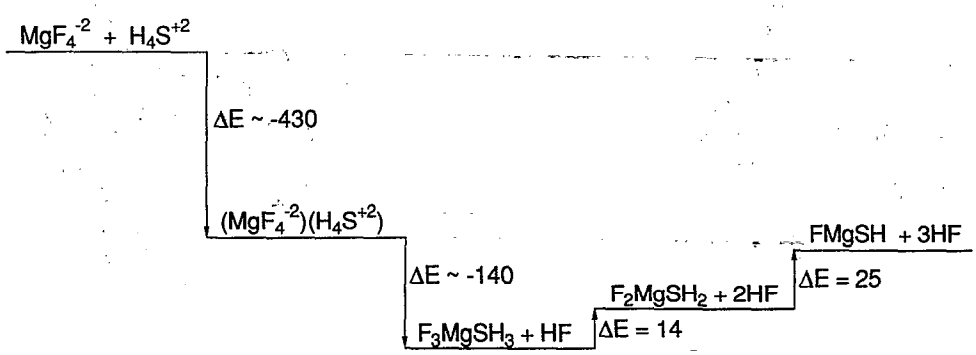

FIG. 7. Energy profile for the rearrangement of the $(F_4Mg^{-2})(H_4S^{+2})$ system.

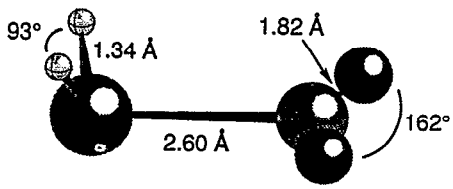

FIG. 8. C_s equilibrium structure of H_2SMgF_2.

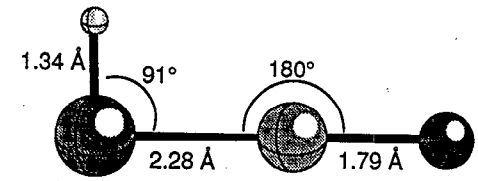

FIG. 9. Equilibrium structure of HSMgF.

Another constrained optimization of H_3SMgF_3 started with both sets of ligands inverted towards one other and produced the structure shown in Fig. 5. Here the ligands are eclipsed, probably due to the strong Coulombic attractions between the H and F centers. This structure is also a second-order saddle point on the potential energy surface, and again the imaginary frequencies (174 cm^{-1}) correspond to a degenerate distortion of the molecule. This isomer lies 20 kcal/mol higher in energy than the minimum energy structure.

The lowest-energy local minimum structure we found for H_3SMgF_3 is shown in Fig. 6 and can be viewed as involving dative interactions among three substructures. This isomer is **not** symmetric. In fact, we carried out a C_s constrained minimization and found an imaginary frequency corresponding to the in-plane antisymmetric stretch of the H_3S portion of the molecule. Distortion along this imaginary frequency mode gave the structure shown in Fig. 6. Calculations on H_2S, MgF_2, and HF revealed that this lowest-energy isomer of H_3SMgF_3 involves three dative interactions among H_2S, HF, and MgF_2 rather than conventional chemical bonds.

The resulting complex has one low-frequency vibration (at 47 cm^{-1}). The bond lengths and angles in the H_2S portion are deformed by 0.02 Å and one degree relative to isolated H_2S; the HF distance is stretched by 0.06 Å relative to HF, and the MgF_2 portion is slightly more deformed, relative to FMgF: 0.04 Å and 30 deg. The Mulliken populations of this structure, as shown in Table VI, quantitatively match those of the three isolated molecules: H_2S, HF, MgF_2, and the molecular orbital LCAO coefficients show evidence for an intact HF bond.

As summarized in Fig. 7, the Coulombic stabilization energy of the contact ion pair $(MgF_4^{-2})(H_4S^{+2})$ is quite large, approximately 430 kcal/mol. Elimination of a single HF molecule to form the first covalently bonded species (H_3SMgF_3) is favored by approximately 140 kcal/mol, although there probably is a significant barrier to elimination analogous to the one shown in Fig. 2. We have not yet identified the transition state for this elimination, but we know the structure of Fig. 6 is a local minimum.

C. Elimination of another HF to form H_2SMgF_2

Also shown in Table VI are data pertinent to the subsequent elimination of another HF molecule to form H_2SMgF_2. This elimination reaction is energetically disfavored by only 14 kcal/mol, and produces the species shown in Fig. 8 whose structure contains no exotic bond lengths or angles. The F–Mg–F portion of this molecule is nearly linear, reflecting the H_2S moiety's perturbation on the MgF_2 framework. This H_2SMgF_2 structure can be thought of as involving a dative bond between H_2S and a linear MgF_2 molecule with a slight geometric distortion of each entity.

D. Further elimination of HF

Elimination of another HF species from H_2SMgF_2 to form HSMgF and HF is endothermic by 25 kcal/mol. The HSMgF structure is shown in Fig. 9 with no unusual bond angles or lengths. The endothermicity of this reaction and that of the preceding reaction lead us to predict that the H_3SMgF_3 triple dative complex is the lowest-energy structure on this potential energy surface.

IV. SUMMARY

Combining the geometrically metastable and electronically stable doubly charged ions H_4S^{+2} and MgF_4^{-2} to form a contact ion pair and subsequent elimination of an HF molecule are both exothermic (by a combined 570 kcal/mol). This leads to the H_3SMgF_3 structure shown in Fig. 6, which we postulate is an adduct involving H_2S, HF, and MgF_2 fragments and is bound by 30 kcal/mol with respect to these three small molecules [found by using our calculated HF and H_3SMgF_3 energies as well as the energies obtained for MgF_2 (−399.147 0676 a.u.) and H_2S (−398.872 2912 a.u.)]. Subsequent loss of one or two HF molecules is endothermic by 14 and 25 kcal/mol, respectively, indicating that H_3SMgF_3+HF is the lowest-energy isomer identified so far on the H_4SMgF_4 potential energy surface.

ACKNOWLEDGMENT

This work was supported by the U. S. National Science Foundation, Grant No. CHE91-16286.

[1] A. I. Boldyrev and J. Simons, J. Chem. Phys. **97**, 4272 (1992).

[2] (a) H. G. Weikert, L. S. Cederbaum, F. Tarantelli, and A. I. Boldyrev, Z. Phys. D **18**, 299 (1991); (b) A. I. Boldyrev and J. Simons, J. Chem. Phys. **97**, 2826 (1992); (c) M. K. Scheller and L. S. Cederbaum, J. Phys. B **25**, 2257 (1992); (d) J. Chem. Phys. **99**, 441 (1993); (e) H. G. Weikert and L. S. Cederbaum, *ibid.* **99**, 8892 (1993); (f) P. Taylor, Mol. Phys. **49**, 1297 (1983). This work details the earliest theoretical study of these cation species.

[3] These species are viewed as prototypes for families of salts in which (i) the cation involves a multiply protonated species whose central atom is more electronegative than H and contains more than one lone pair of electrons (e.g., S, O, Se, F, Cl, etc.) and (ii) the anion's central atom is less electronegative than the ligands attached to it and contains two or more empty orbitals to act as Lewis acid sites for negatively charged ligands (e.g., Mg, Ca, B, Al, Ga, etc.). Which particular ion pairs are of most interest to examine will depend on the ionic radii of the positive and

negative ions; only when these radii are proper will efficient packing into favorable crystal structures be possible.

[4]The sizes of the positive MH_n^{2+} and negative $M'X_{n'}^{2-}$ ion moieties are also important here; if M and M′ are too different in size, the M–M′ bond will be weak, and if X is too large, steric crowding of the M–M′ bond will occur.

[5](a) R. Krishnan, J. S. Binkley, R. Seeger, and J. A. Pople, J. Chem. Phys. **72**, 650 (1980); (b) M. J. Frisch, J. A. Pople, and J. S. Binkley, *ibid.* **80**, 3265 (1984); (c) T. Clark, J. Chandrasekhar, G. W. Spitznagel, and P. v. R. Schleyer, J. Comput. Chem. **4**, 294 (1983); (d) A. D. McLean and G. S. Chandler, J. Chem. Phys. **72**, 5639 (1980).

[6]M. J. Frisch, G. W. Trucks, M. Head-Gordon, P. M. Gill, M. W. Wong, J. B. Foresman, B. G. Johnson, H. B. Schlegel, M. A. Robb, E. S. Replogle, R. Gomperts, J. L. Andres, K. Raghavachari, S. Binkley, C. Gonzalez, R. L. Martin, D. J. Fox, D. J. DeFrees, J. Baker, J. J. P. Stewart, and J. A. Pople, GAUSSIAN92, Revision C (Gaussian, Pittsburgh, PA, 1990).